Evidence of the effect of summertime midlatitude convection on the subtropical lower stratosphere from CRYSTAL-FACE tracer measurements

Eric A. Ray,[1,2] Karen H. Rosenlof,[1] Erik C. Richard,[1,2] P. K. Hudson,[1,2] D. J. Cziczo,[1,2] M. Loewenstein,[3] H.-J. Jost,[3] J. Lopez,[3] B. Ridley,[4] A. Weinheimer,[4] D. Montzka,[4] D. Knapp,[4] S. C. Wofsy,[5] B. C. Daube,[5] C. Gerbig,[5] I. Xueref,[5] and R. L. Herman[6]

Received 16 February 2004; revised 21 May 2004; accepted 18 June 2004; published 18 September 2004.

[1] Trace gas and particle measurements taken during the CRYSTAL-FACE mission are used to examine mixing in the summer subtropical lower stratosphere. Vigorous convection in the central and eastern United States injected a significant amount of tropospheric air into the lower stratosphere, which was subsequently advected over the region sampled during the CRYSTAL-FACE mission. Aerosols produced by biomass burning were observed over Florida during a time period with a large number of forest fires in the western United States and eastern Canada, providing evidence of convective injection of tropospheric air into the lower stratosphere. The circumstances of the large-scale flow pattern in the upper troposphere and lower stratosphere, vigorous summertime convection, abundant forest fires, and the downstream sampling allow a unique view of mixing in the lower stratosphere. We calculate the fractions of midlatitude tropospheric air in the sampled lower stratosphere and mixing rates on the basis of consistency between a number of tracer-tracer correlations. The tropospheric endpoints to the mixing estimates give an indication of midlatitude continental convective input into the lower stratosphere. We also discuss the possible impact of summertime midlatitude convection on the composition of the stratosphere as a whole. *INDEX TERMS:* 0341 Atmospheric Composition and Structure: Middle atmosphere—constituent transport and chemistry (3334); 0368 Atmospheric Composition and Structure: Troposphere—constituent transport and chemistry; 3314 Meteorology and Atmospheric Dynamics: Convective processes; 3334 Meteorology and Atmospheric Dynamics: Middle atmosphere dynamics (0341, 0342); 3362 Meteorology and Atmospheric Dynamics: Stratosphere/troposphere interactions; *KEYWORDS:* convection, mixing, stratosphere

Citation: Ray, E. A., et al. (2004), Evidence of the effect of summertime midlatitude convection on the subtropical lower stratosphere from CRYSTAL-FACE tracer measurements, *J. Geophys. Res.*, *109*, D18304, doi:10.1029/2004JD004655.

1. Introduction

[2] The mixing of air in the lowermost stratosphere has important implications for a variety of processes in the UT/LS. The different pathways by which air enters the lowermost stratosphere create an environment of distinct air masses that mix together on a range of spatial and temporal scales. In particular, exchange between the very different air masses of the stratosphere and troposphere leads to large gradients in chemical species. The chemical and radiative balance of the UT/LS is greatly impacted by this exchange and mixing [e.g., *Esler et al.*, 2001]. Since the range of spatial scales on which mixing occurs is quite large, it is difficult to measure or model this region with enough resolution or spatial sampling to completely describe the mixing processes.

[3] The injection of tropospheric air into the lower stratosphere by subtropical or midlatitude convection is a process whose effects on the stratosphere are not well known. This is primarily due to the short time and small spatial scales on which convection occurs and the small percentage of convective events vigorous enough to penetrate into the stratosphere. These characteristics make convective influence on the stratosphere difficult to directly measure or model. Basic questions on the role of deep convection in the dehydration of the stratosphere are still not fully understood. The effects of convection are of fundamental importance in the tropics, where air is lifted into the upwelling region of the stratosphere. However, it is less clear what impact vigorous convection in the subtropics and midlatitudes, associated with monsoon circulations for instance, has on the composition of the stratosphere as a whole.

[1]NOAA Aeronomy Laboratory, Boulder, Colorado, USA.
[2]Also at Cooperative Institute for Research in Environmental Sciences, University of Colorado, Boulder, Colorado, USA.
[3]NASA Ames Research Center, Moffett Field, California, USA.
[4]National Center for Atmospheric Research, Boulder, Colorado, USA.
[5]Department of Atmospheric Sciences, Harvard University, Cambridge, Massachusetts, USA.
[6]Jet Propulsion Laboratory, Pasadena, California, USA.

0148-0227/04/2004JD004655

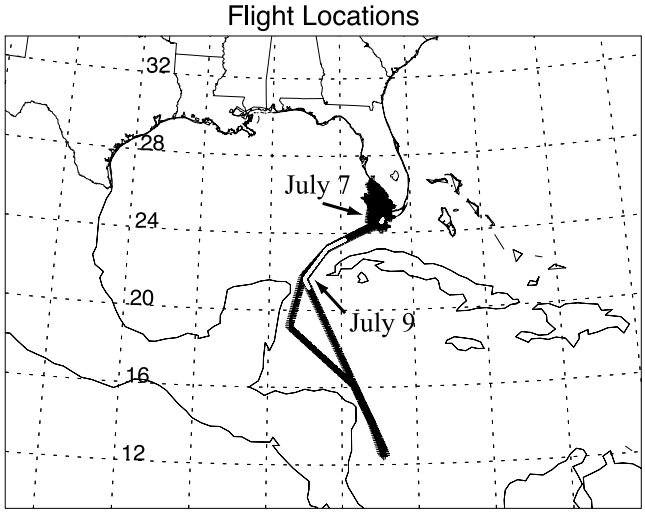

Figure 1. Flight tracks of the WB-57F for 7 and 9 July 2002. The white center of the track indicates the regions where the plumes of CO, NO_y, and biomass burning particles were measured.

[4] To describe the extratropical convective influence on the stratosphere, it is necessary to know both how much air is input by convection into the stratosphere as well as the fate of the injected air. The first of these processes is quite difficult to determine since there are multiple pathways by which air enters the extratropical lower stratosphere. It has been known, but perhaps not fully appreciated, for many years that midlatitude convection can penetrate well into the lower stratosphere [*Roach*, 1967]. Chemical signatures of tropospheric air have often been measured in the subtropical and midlatitude lower stratosphere [*Hoor et al.*, 2002; *Ray et al.*, 1999; *Hintsa et al.*, 1998], but convection was not thought to be the process that caused many of these observed stratospheric perturbations. Observational studies that have inferred convective injection of tropospheric air into the lower stratosphere made use of specific short-lived in situ trace gas measurements [e.g., *Jost et al.*, 2004; *Fischer et al.*, 2003; *Tuck et al.*, 1997] or satellite aerosol measurements [*Fromm and Servranckx*, 2003; *Fromm et al.*, 2000]. Recently, there also have been high-resolution modeling studies that have begun to resolve detailed convective transport in the UT/LS [e.g., *Wang*, 2003].

[5] The impact and fate of the convectively injected air in the extratropical lower stratosphere are affected by the background flow, radiative heating rates and the rate of mixing with background stratospheric air. The climatological stratospheric flow during the monsoon season can result in extensive southward advection of mid and high latitude stratospheric air into the subtropics [*Dunkerton*, 1995]. Radiative heating rates equatorward of roughly 30° latitude above 360 K are positive [*Rosenlof*, 1995]. This suggests that air injected into the stratosphere above the 360 K level either at latitudes less than 30°, or at latitudes higher than 30° and subsequently advected to lower latitudes, will rise and spread throughout the stratosphere. The rate with which the tropospheric air is mixed with the surrounding stratosphere can also have a chemical and radiative impact on the extratropical lower stratosphere [e.g., *Esler et al.*, 2001].

[6] The purpose of this paper is to estimate the amount of mixing of convectively injected tropospheric air with the surrounding lower stratosphere based on measurements taken during the CRYSTAL-FACE mission in July 2002. Two flights in particular, 7 and 9 July, passed through layers of air in the lower stratosphere which contained highly perturbed chemical and particle compositions compared to the surrounding stratosphere. Highly elevated CO, CO_2 and NO_y along with particle signatures typical of biomass burning suggest a recent injection of tropospheric air into the lower stratosphere. Trajectories indicate that equatorward large-scale flow in the lower stratosphere transported air from the vigorous convective region of the central and eastern United States and Canada, where forest fires were present, to the sampled region. We will calculate mixing fractions, mixing rates and estimate the boundary conditions for tropospheric air convectively injected into the stratosphere based on the flights of 7 and 9 July. These quantities are of interest since there have been very few in situ measurements in the stratosphere that can help describe mixing of such distinct air masses from known sources over a timescale of 5–10 days.

2. Measurements

[7] The NASA CRYSTAL-FACE mission took place from 29 June to 31 July 2002 based out of Key West, Florida. The main purpose of the mission was to characterize cirrus clouds in the vicinity of tropical convection. The measurements used in this paper were taken on the WB-57F aircraft, which can fly in the upper troposphere and lower stratosphere up to roughly 20 km. Measurements of O_3 [*Proffitt and McLaughlin*, 1983], NO_y [*Ridley et al.*, 1994], CO [*Loewenstein et al.*, 2002], CO_2 [*Daube et al.*, 2002], particles from the PALMS instrument [*Murphy et al.*, 1998] and pressure and temperature [*Thompson and Rosenlof*, 2003] are used. All of these measurements were taken by fast response, typically 1 Hz, high precision instruments.

[8] The flights discussed in this paper took place on 7 and 9 July 2002. The flight of 7 July was local to Key West with a track entirely over the southwestern portion of Florida (Figure 1). The flight of 9 July was a southern survey flight which had a track through the Gulf of Mexico, south to approximately 12°N and back to Key West.

3. Results

3.1. Large-Scale Stratospheric Flow and Tropospheric Conditions During July 2002

[9] The large-scale flow in the lower subtropical stratosphere during July 2002 was dominated by a region of high pressure situated over the south central United States [*Richard et al.*, 2003]. This flow pattern is typical of the summertime North American monsoon circulation. The region of high pressure resulted in northerly flow over the southeastern United States and Caribbean in the pressure range of 100–200 hPa, or potential temperatures of roughly 350–400 K. Above 400 K the stratospheric flow was easterly during the entire month of July. This flow pattern produced a "wedge" shaped air mass with mid and high latitude lower stratospheric characteristics over the southeastern United States and Caribbean between 350 and 400 K

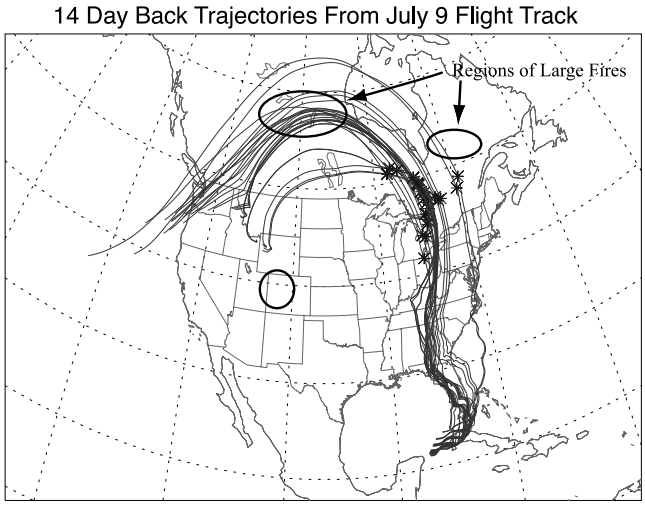

Figure 2. A map of 14 day back trajectories calculated by FLEXTRA using NCEP AVN assimilated model output. The trajectories were initialized at roughly 30 s intervals along the portions of the 9 July flight track where the "plume" was located. Asterisks denote the trajectory positions after 10 days. The ellipses encompass regions of significant fire activity during late June and early July 2002 as determined by MODIS (modis-fire.gsfc.nasa.gov/).

with a sharp transition above 400 K to tropical lower stratospheric conditions. The "wedge" shape was due to the erosion of the northerly flow at lower latitudes, mostly from the easterly flow above, so that the air mass thinned toward lower latitudes. One of the effects of this large-scale flow pattern was to transport lower stratospheric air from the midlatitude United States and Canada to the subtropical latitudes sampled during CRYSTAL-FACE.

[10] The forest fire season in the western United States and Canada during 2002 happened to be one of the most active in the last 50 years. Major fires occurred in June in Colorado, Arizona and Saskatchewan and in early July in Quebec. These fires spread an extensive pall of smoke over large regions of the central and eastern United States and Canada from late June to early July. Thus a strong convective event in this region that penetrated the lower stratosphere would be expected to significantly perturb the stratosphere downstream of the fires with a chemical and particulate signature of biomass burning.

[11] Signatures of biomass burning in the lower stratosphere have been seen previously in satellite aerosol measurements [*Fromm and Servranckx*, 2003; *Fromm et al.*, 2000] and from in situ measurements [*Waibel et al.*, 1999; *Lelieveld et al.*, 1997]. The flights of 7 and 9 July 2002 during CRYSTAL-FACE exhibit regions of significant chemical and particle perturbations in the lower stratosphere consistent with the effects of biomass burning [*Jost et al.*, 2004]. These perturbations include elevated CO and other trace gases as well as particle measurements sampled by PALMS that are similar in composition to those sampled previously in smoke plumes [*Hudson et al.*, 2004]. Figure 1 indicates the parts of the flight track where biomass burning particles were sampled as well as very high CO and NO_y mixing ratios, hereafter referred to as the "plume" air mass.

[12] So how did this plume air mass get transported into the stratosphere? The two most common methods of transport from the troposphere to the stratosphere in the extratropics are quasi-isentropic exchange and convective overshooting. There is compelling evidence to suggest that the sampled plume was injected by a convective event or events downstream of fires in Canada or the western United States. Figure 2 shows 14 day back trajectories initialized on the 9 July flight track at locations where the plume was sampled. These trajectories pass over and near several regions of significant biomass burning as indicated by the ellipses in Figure 2. *Jost et al.* [2004] have also examined the source of the plume using in situ measurements, model back trajectories and satellite aerosol data. They found that a strong convective event in Saskatchewan was most likely to have injected air into the stratosphere near the region of forest fires. The trajectories calculated in the work of *Jost et al.* [2004] agree very closely to those shown here but we are not sufficiently confident in the trajectories to identify a particular convective event responsible for the plume.

[13] The strongest evidence for convective injection of tropospheric air comes from the PALMS particle data. Over 95% of the particles in the plume were classified as of biomass origin. This large fraction of biomass burning particles measured in the plume suggests a relatively unmixed, and thus recent injection of tropospheric air into the stratosphere. The absence of tropospheric material such as mineral dust, sulfates, etc. other than biomass in the plume also indicates the air mass was injected into the stratosphere very close to the source fires. A much smaller fraction, 45–50%, of particles outside of the plume are classified as having biomass origin. This fraction of particles outside of the plume in the lower stratosphere is still quite high, which suggests that there was a significant amount of transport of tropospheric air into the extratropical lower stratosphere during this time period. As mentioned above, quasi-isentropic mixing also likely transported air with biomass burning characteristics into the lower stratosphere since the fires spread smoke into the middle and upper troposphere over a large region. However, dispersion and mixing in the troposphere is much more efficient than in the stratosphere so the high fraction of biomass burning particles and the overall number of particles measured in the plume indicate that it experienced little mixing in the troposphere prior to the exchange into the stratosphere.

[14] The strong evidence for recent (on the order of 10 days prior to the sampling) convective injection of the plume is important since it allows us to perform a mixing calculation assuming the endpoints are the background stratosphere and the convectively injected plume. It is rare to be able to identify an air mass in the lower stratosphere with a distinct origin such as from a convective event. By doing so, we can examine the rate of mixing of the plume with the background stratosphere as well as the composition of the convectively injected air mass. Exactly where the sampled biomass burning particles and associated tropospheric air originated and which convective system(s) injected this air into the stratosphere cannot be definitively determined here. However, the mixing calculations performed here are not dependent on knowledge of the origination fires. The important point is that the biomass burning particle and anomalous chemical measurements

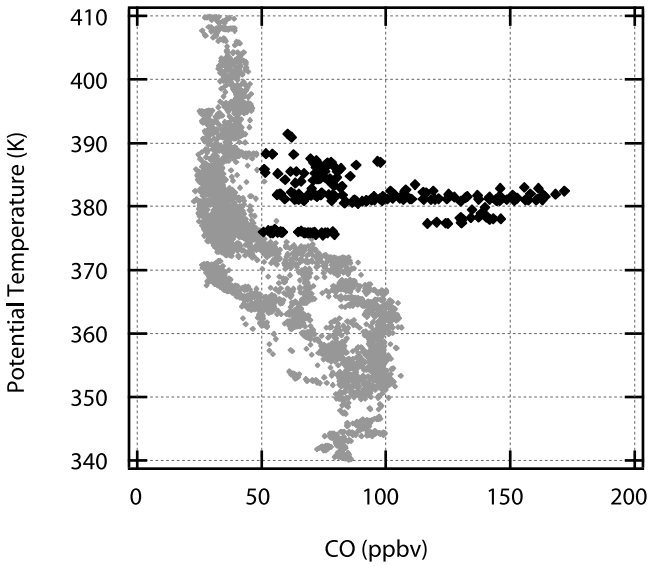

Figure 3. Profile of CO versus potential temperature for the 9 July 2002 WB-57F flight. Light shaded points indicate data from the entire flight and dark shaded points are in the "plume" portion of the flight as discussed in the text.

reveal that there was recent injection of tropospheric air into the lower stratosphere from at least one midlatitude convective event.

[15] An interesting feature of the measurements in the lower stratosphere is the high potential temperatures where biomass burning particles and anomalous trace gas mixing ratios were observed. Figure 3 shows CO measurements from the 9 July flight as a function of potential temperature with the plume region highlighted. The majority of the points in the plume are between 375 and 390 K. Radiative heating rates are small in this part of the stratosphere so diabatic motion over the course of one week would only be on the order of several degrees. This implies that the convection, and associated gravity wave activity, was vigorous enough to inject air up to potential temperatures of greater than 380 K. The local tropopause over the eastern United States was 350–360 K so the convection penetrated well above the local tropopause. The study by *Roach* [1967] using observations from the ER-2 discussed cloud tops over the midwestern United States that reached up to 6 km above the local tropopause. Recent modeling work by *Wang* [2003] suggests that midlatitude convection can penetrate well above the tropopause and deposit a plume of tropospheric air into the lower stratosphere aided by the presence of gravity wave breaking. The level to which midlatitude convection can penetrate the lower stratosphere may have important implications for the impact on the stratosphere as a whole. This topic will be discussed further below.

3.2. Lower Stratospheric Isentropic Mixing

[16] The transport and mixing processes assumed to have occurred prior to the sampling of the lower stratosphere on 7 and 9 July 2002 are summarized in the schematic shown in Figure 4. Tropospheric air with particles from biomass burning, high CO and NO_y and low O_3 mixing ratios was injected by a vigorous midlatitude convective event or perhaps more than one event into the lower stratosphere. This tropospheric air is then assumed to have mixed isentropically with the surrounding stratosphere at some rate that was dependent on the shear of the flow as it was advected southward into the sampled region in the subtropics. In this section we will focus on the isentropic mixing that occurred in the lower stratosphere following the convection.

[17] To quantitatively examine the mixing between the plume and the lower stratosphere we use correlations between several long-lived trace gases. The only processes that can cause a change in the correlation between two trace gases are local chemistry and mixing between air masses with very distinct chemical compositions [*Plumb and Ko*, 1992]. Local chemical lifetimes of O_3, NO_y, CO and CO_2 in the extratropical lower stratosphere are long compared to the transport timescale in this region, which is on the order of weeks [*Brasseur and Solomon*, 1986]. However, it is likely that the perturbed chemical environment of the plume resulted in anomalous photochemistry in the lower stratosphere. Studies of photochemistry within biomass burning plumes suggest that above 12 km the lifetime of CO is 1–2 months [*Mauzerall et al.*, 1998]. Many studies have also calculated enhancements of a variety of trace gases relative to CO and CO_2 within biomass plumes [e.g., *Ryerson et al.*, 2001; *Andreae et al.*, 2001; *Mauzerall et al.*, 1998]. Photochemical modeling work of conditions in the lower stratosphere similar to those in the plume indicate that O_3 production could have occurred at a much higher rate than in typical lower stratospheric conditions, but that CO, CO_2 and NO_y were essentially inert (K. Drdla, personal communication, 2004). We use the biomass plume enhancement ratio of O_3 relative to CO calculated in previous studies to estimate the O_3 production within the plume based on the measured CO enhancement. We account for a range of O_3 production within the plume in the mixing calculation but assume that the other tracers remained inert throughout the 7–12 day transport timescale in the lower stratosphere.

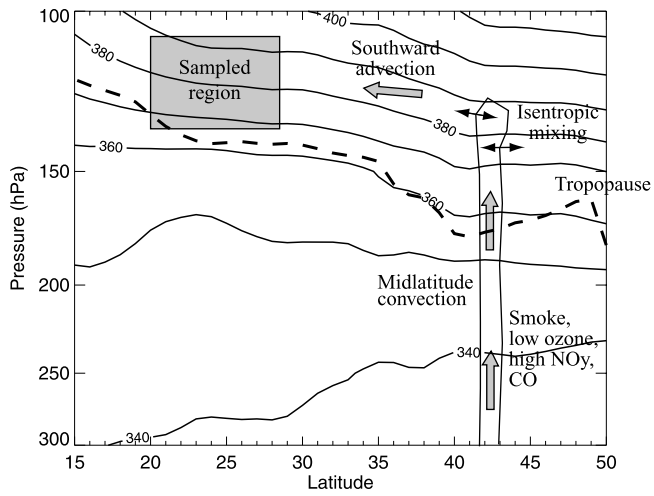

Figure 4. Schematic of the transport of tropospheric air into the sampled region of the lower stratosphere. The latitude-pressure cross section of potential temperature and tropopause height are from NCEP analysis on 7 July 2002, 06Z at a longitude of 78°E. The convection is assumed to have occurred in the midlatitudes over the continental United States several days before the WB-57F sampled the lower stratosphere over Key West, Florida.

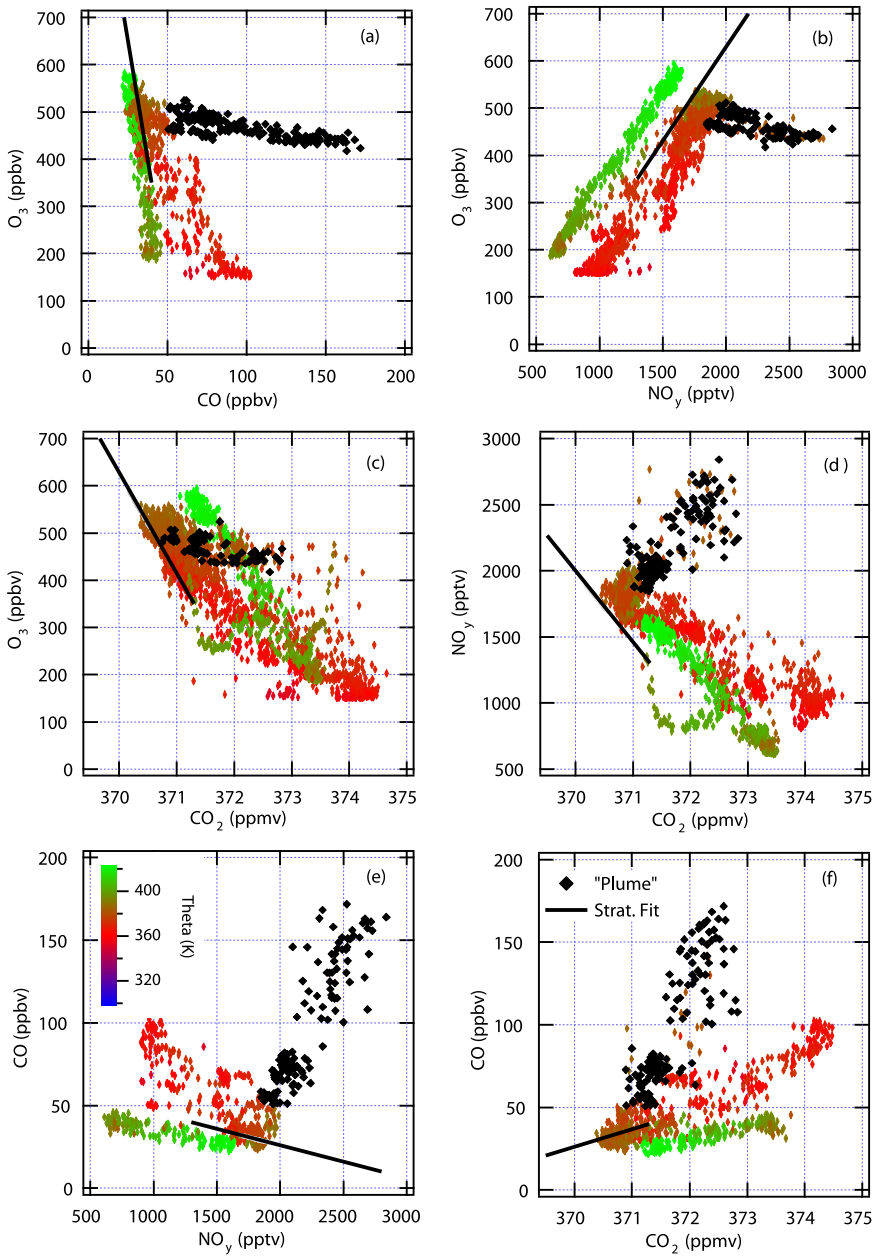

Figure 5. Correlation plots of all the long-lived tracers for the 9 July 2003 flight. The light shaded points are all the measurements taken above potential temperatures of 350 K and ozone mixing ratios of 150 ppbv. The black points are in the smoke plume and are used in the mixing calculation described in the text. The solid black line is an estimate of the typical midlatitude correlation in the lower stratosphere and is used as an end point in the mixing calculation.

[18] Correlations between O_3, CO, CO_2 and NO_y for the 9 July 2002 flight are shown in Figure 5. The measurements are color coded by potential temperature to help differentiate the distinct stratospheric regions that were sampled during this flight. The green shaded points ($\theta > 400$ K) have relatively low CO and NO_y mixing ratios and relatively high CO_2 mixing ratios, which is consistent with a mostly subtropical stratospheric air mass. The points with a red shading (390 K $> \theta >$ 350 K) have relatively high CO and NO_y mixing ratios and relatively low CO_2 mixing ratios consistent with the mid to high latitude lower stratospheric wedge air mass. The black points highlight the plume region, which has a significantly different correlation slope in each plot of Figure 5 compared to either the subtropical or mid to high latitude lower stratosphere. The highly elevated CO and NO_y mixing ratios are consistent with the effects of biomass burning as discussed earlier. The linear shape of the plume correlation in each plot is suggestive of a mixing line between a convectively injected air mass from the troposphere and a background stratospheric air mass. The solid lines on each plot represent an estimate of the typical midlatitude lower stratosphere correlations based primarily on previous aircraft measurements [*Fahey et al.*, 1996; *Hoor et al.*, 2002].

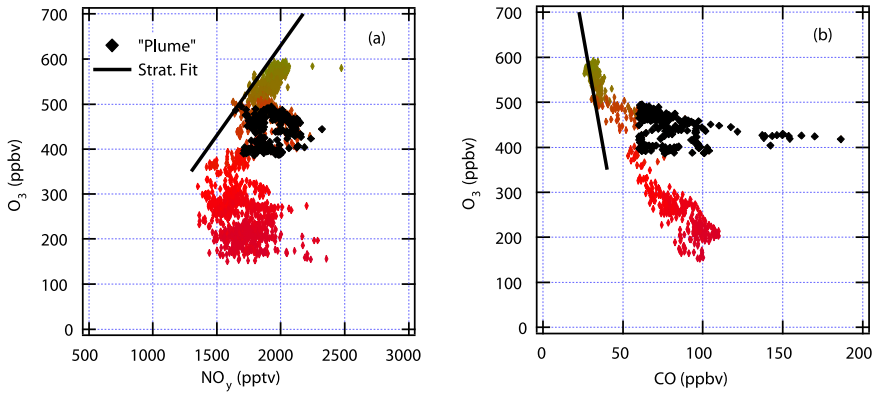

Figure 6. Correlation plots of the long-lived tracers for the 7 July 2002 flight. Color shading is the same as in Figure 5.

[19] The long-lived tracer correlations from the flight of 7 July (Figure 6) are similar to those of 9 July. The WB-57F only sampled potential temperatures up to about 390 K so the subtropical correlations seen on 9 July are not present on 7 July. In the wedge region of the lower stratosphere and in the plume the correlations are similar between the two flights, although the plume correlation is much less pronounced in the O_3-NO_y correlation on the 7 July flight. Measurements of CO_2 were not taken on this flight so only correlations between O_3, CO and NO_y are shown and used in the mixing calculation. An interesting question is how much, if any, of the plume sampled on 7 July is the same plume as that sampled on 9 July. The very similar correlations in the plume, particularly between O_3 and CO, and the similar potential temperature range suggests that at least part of the plume sampled on 7 July was the same air mass as that sampled on 9 July. Trajectories initialized on the 7 July flight track (not shown) indicate that the air in the 375–390 K range moved to the southwest over the region of the 9 July flight track where the plume was sampled. The part of the plume sampled between 365 and 375 K on 7 July was likely advected to the south and southeast due to vertical shear in the wind direction. Support for the trajectory analysis comes from the lack of measurements sampled below 375 K on 9 July that show significant deviations from the correlations in the wedge region. This lack of plume measurements at lower potential temperatures on 9 July is not due to a lack of sampling since at locations north of 20°N most measurements were taken in the 360–380 K range. Thus if the plume did extend below 375 K it would have been sampled. This indicates that the plume had a sharp lower boundary due to the shear of the background flow. Thus the same plume air mass was likely sampled during both flights in the 375–390 K potential temperature range, but the plume below 375 K was advected in a different direction following the 7 July flight. The similar spatial proximity of the plume sampled above and below 375 K on 7 July is suggestive that all of the plume air mass is a result of the same convective event.

[20] The goal of the first part of the mixing calculation is to determine the fraction of tropospheric air in the plume air mass. To calculate the fraction of tropospheric air we use the plume tracer correlations shown in Figures 5 and 6, and assume these correlations resulted from mixing between the background stratospheric correlations and the convectively input tropospheric correlations. The use of tracer correlations to quantify mixing has been used in previous studies [e.g., *Plumb et al.*, 2002; *Ray et al.*, 2002], but in this calculation we include photochemical production of O_3 as well as mixing. Figure 7 shows a schematic example of the mixing calculation for O_3 versus CO and how the O_3 production

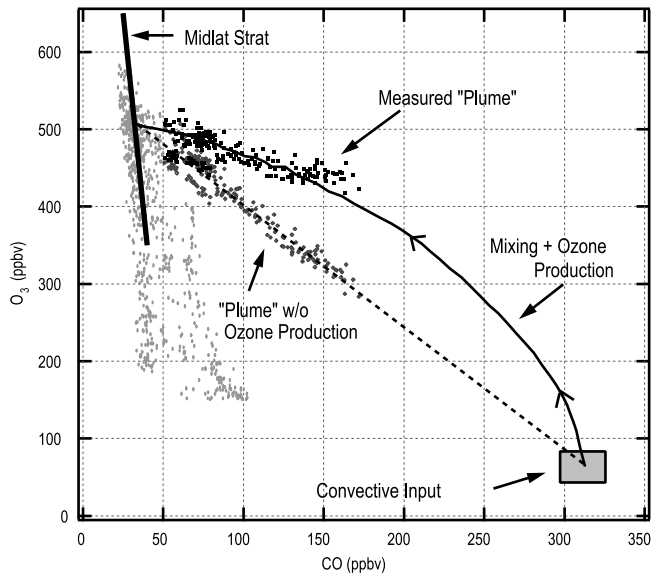

Figure 7. A schematic of the mixing lines for the case of the O_3 versus CO correlation. The mixing is assumed to have occurred between the convectively injected tropospheric air, represented by the gray box, and the background midlatitude stratospheric air, represented by the solid black line. In the mixing calculation performed here, the mixing lines were allowed to pivot around the plume correlation, adjusted for photochemical O_3 production, in order to match the mixing fraction for all tracer pairs. Thus the convective boundary conditions and midlatitude stratospheric mixing ratios were allowed to vary within certain observational constraints described in the text. The data labeled "plume w/o ozone production" are not actual measurements but rather are plume measurements adjusted for the amount of O_3 production assumed to have occurred in the stratosphere. The O_3 production shown here represent the highest values assumed in the calculation.

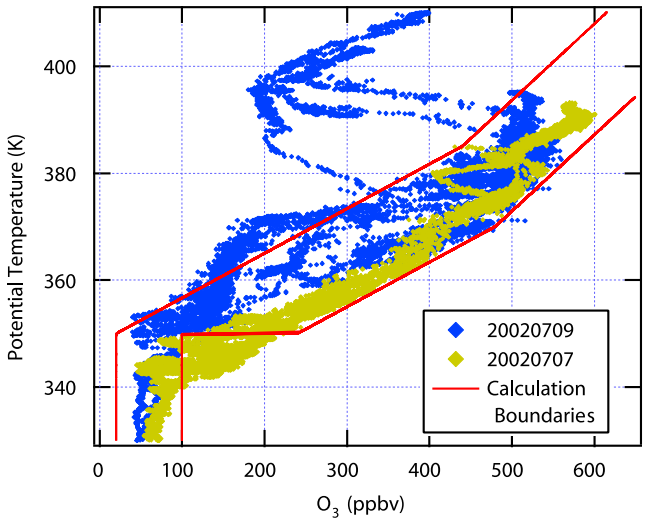

Figure 8. Profiles of O_3 as a function of potential temperature from the 7 and 9 July 2002 flights. The O_3 minimum and maximum profiles used in the mixing calculation are shown by the solid red lines.

impacts the calculation. The endpoints of the mixing calculation are the convective input, which is the origination of the plume air mass, and the midlatitude stratosphere. Over time the plume mixes with the surrounding stratosphere, which moves the plume correlations toward the midlatitude stratosphere correlations, and O_3 is produced, which moves the correlations only toward higher O_3 mixing ratios. The result is a curving path on the correlation plot, moving toward lower CO and higher O_3 mixing ratios. Each measurement in the plume had a unique mixing and O_3 production path that occurred over the previous 7–12 days and ended at the measurement location on the correlation plot at the time of observation. The effect of the O_3 production is to elevate the O_3 mixing ratios in the plume. Without O_3 production the plume correlations would have looked something like the light gray points in Figure 7. For the mixing calculation we account for the O_3 production by reducing the O_3 in the plume and then assume a linear mixing line between the reduced O_3 plume and the mixing endpoints as denoted by the dashed line in Figure 7. The O_3 production is scaled by the measured CO enhancement above the background UT/LS mixing ratios. The correlations with the highest CO mixing ratios are thus assumed to have spent the most time in the chemically perturbed biomass burning conditions where O_3 is more efficiently produced. The effect of removing the O_3 production in this way is to rotate the plume correlations such that the correlations with lower CO mixing ratios change their O_3 mixing ratios less than the correlations with higher CO mixing ratios. This changes the slope of the plume correlations as shown in Figure 7.

[21] The fraction of tropospheric air in the stratosphere is calculated for each tracer correlation from the following equation:

$$F_{trop}(i) = \frac{\sqrt{(\chi_1(i) - \chi_{1strat}(i))^2 + (\chi_2(i) - \chi_{2strat}(i))^2}}{\sqrt{(\chi_{1strop}(i) - \chi_{1strat}(i))^2 + (\chi_{2strop}(i) - \chi_{2strat}(i))^2}}, \quad (1)$$

where $\chi_1(i)$ and $\chi_2(i)$ are plume mixing ratios, adjusted for O_3 production, at a particular point i, $\chi_{1trop}(i)$ and $\chi_{2trop}(i)$ are the convective boundary conditions and $\chi_{1strat}(i)$ and $\chi_{2strat}(i)$ are the midlatitude stratospheric boundary conditions. We assume the convective boundary condition for O_3 is fixed and that initially the midlatitude stratospheric O_3 mixing ratio for a particular potential temperature is in the middle of the observed range shown in Figure 8. From the initial stratospheric O_3 mixing ratio we can find the initial stratospheric mixing ratio for each other tracer based on the midlatitude stratospheric correlation lines shown in Figure 5. From these initial values of χ_{1strat} and χ_{2strat} we can calculate the initial convective boundary condition for each tracer as the point where the mixing line between the stratospheric endpoint and the plume correlation intersects the O_3 convective boundary condition as shown by the dashed line in Figure 7.

[22] The only physically realistic solution is for each of the tropospheric fractions in the plume to be the same for all of the tracer correlations since the mixing process is identical. So after the tropospheric fractions are calculated for all of the points in the plume for each of the tracer correlations using the initial stratospheric and convective input boundary conditions, an iteration is performed to solve for fractions that are consistent among all of the tracer correlations. Since the most uncertain quantity is the convective input, we chose to adjust the stratospheric boundary condition in the iteration. The stratospheric boundary condition is constrained by the midlatitude correlation as well as the measured profiles of O_3 versus potential temperature. Figure 8 shows measured O_3 versus potential temperature for the flights of 7 and 9 July. An O_3 profile from Wallops Island, VA (not shown) taken on 3 July is very similar to the 7 July O_3 profile measured over Florida. This is consistent with the southward flow in the lower stratosphere along the east coast of the United States during this period and the push of high O_3 from the midlatitudes into the subtropics. By contrast, ozonesonde measurements over Boulder, Colorado during this period showed very little enhancement over normal lower stratospheric values, and were considerably lower than the values measured over Wallops Island and Florida. Thus we can set limits on the maximum and minimum O_3 mixing ratios as a function of potential temperature as shown by the solid lines in Figure 8.

[23] To perform the iteration we first adjusted the stratospheric boundary O_3 mixing ratio toward a higher (lower) value to give a larger (smaller) tropospheric fraction. The adjustment of the stratospheric O_3 mixing ratios was constrained by the O_3 profile. From the midlatitude stratospheric correlations we used the new O_3 mixing ratios to adjust the other stratospheric tracer boundary conditions. The new stratospheric endpoints are used to define new mixing lines, which result in different mixing fractions and tropospheric endpoints. The iteration is performed several times and the mixing fractions for all of the correlation pairs agree to within less than a tenth of a percent.

[24] The fractions of tropospheric air calculated from the tracer correlations are shown as a function of potential temperature in Figure 9. The region between roughly 377 and 383 K has the largest fractions, with values from 0.2 up to 0.45, and the values are similar for both flights. This is consistent with the idea mentioned above that the same

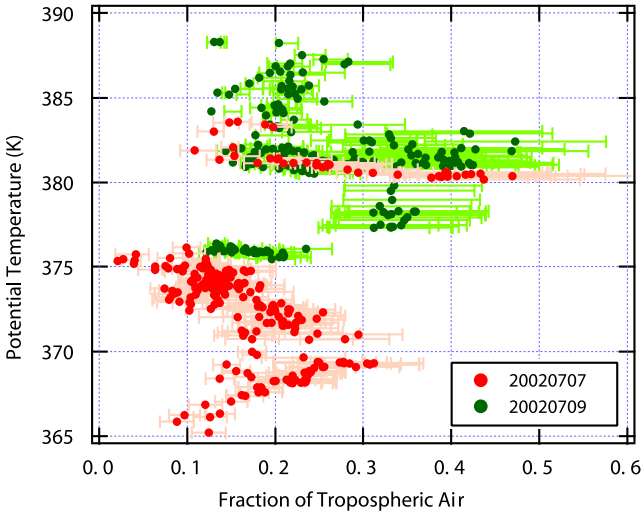

Figure 9. Fraction of tropospheric air in the "plume" air masses sampled in the lower stratosphere. The fractions were calculated using the tracer correlations as described in the text. Error bars were calculated from uncertainties in the ozone versus potential temperature profile (Figure 8), stratospheric boundary condition correlations, and tropospheric ozone mixing ratios.

plume air mass was sampled during both flights. Above 383 K and below 377 K the fractions are between 0.1 and 0.3 and are again similar for both flights. So the mixing calculation indicates that a layer of the plume maintained a significant tropospheric characteristic even after a week or more in the stratosphere. The plume above and below this layer mixed more efficiently with the surrounding stratosphere. Vertical inhomogeneities in the turbulent mixing during convection or wind shear variability during the subsequent advection in the lower stratosphere may have contributed to the vertical gradient in the calculated mixing fractions.

[25] The calculated fractions of tropospheric air in the stratosphere reveal some information about the timescale of mixing in the lower stratosphere. We can quantify a mixing rate by simply dividing the fraction of stratospheric air in the plume, which is 1-*F*, by an estimate of the time between the convective event and the sampling. As an example, if we assume the plume was injected into the stratosphere within the last 7–12 days, for $F = 0.25$ the mixing rate has a range of 6–10%/day. There are, of course, some large uncertainties in the mixing process, primarily in the initial conditions during the convective events. We included a range of timescales from 7–12 days since we do not know when the convective event or events occurred. It is possible that the convective injection occurred prior to 12 days before the plume was sampled. However, based on trajectory calculations, it is highly unlikely that the plume was injected more than 14 days prior to sampling since air in the lower stratosphere was advected across North America within that time frame. Since the only highly concentrated sources of biomass burning particles were in the United States and Canada, the transit timescale across the continent acts as a constraint on the mixing timescale.

[26] Error bars on the calculated fractions are estimated from several sources of uncertainty added in quadrature. The primary sources of errors result from uncertainties in the O_3 production rate, the midlatitude stratospheric correlation and the tropospheric O_3 mixing ratio. The tropospheric O_3 mixing ratio for the base calculation was chosen to be 75 ppbv and for the error calculation an uncertainty range of 50–100 ppbv was used. The midlatitude stratospheric correlation was changed by a few percent around the correlations shown in Figure 5 to represent uncertainty in the correlation. This resulted in the smallest uncertainty in the mixing calculation. The O_3 production rate was estimated by using the $\Delta O_3/\Delta CO$ enhancement ratio calculated in previous studies of biomass burning plumes as mentioned earlier. For the base case we assumed $\Delta O_3/\Delta CO = 0.7$, with 0.3 and 1.1 used for the lower and higher estimates of ozone production. These values represent some of the uncertainty quoted in previous studies as well as the lack of previous studies of biomass burning plume characteristics in the stratosphere.

[27] Another uncertainty that was not quantified in the mixing calculation is the amount of mixing that took place as the convection penetrated the stratosphere. It is likely that during the convective penetration of air into the lower stratosphere there was some amount of mixing on a short timescale. This would result in an air mass that, on the timescale of hours, contained some amount of tropospheric air mixed with the surrounding stratospheric air. The mixing associated with the turbulence of convection is different from the diffusive and shear induced mixing that occurred downstream of the convection in the lower stratosphere. The notion that a significant amount of mixing occurred in a short period of time during the convection is supported by the similarity in the calculated fractions above 380 K between the two flights (Figure 9). These flights were separated by two days and, as mentioned previously, we assume that the same plume air mass above 380 K was sampled on both flights. Since the fractions are approximately the same on 7 July as those two days later this suggests only a small amount of mixing occurred in this time period. A caveat is that a much smaller portion of the plume was sampled on 7 July compared to 9 July. Unfortunately we have no way of estimating the amount of turbulent mixing in the lower stratosphere associated with the convection, and modeling studies are only beginning to resolve this process [e.g., *Lane et al.*, 2003]. Thus the mixing rate is likely to be considerably smaller than that calculated above. We could convert the mixing rate into a diffusion coefficient using an estimate of the plume size but the number would be highly uncertain and likely an overestimate since it would include turbulent as well as diffusive mixing.

3.3. Composition and Mass of Air Injected by Convection Into the Lower Stratosphere

[28] In the calculation of the tropospheric mixing fraction described above, the convective boundary condition was essentially allowed to freely vary in order to iterate to a fraction of tropospheric air that was consistent among all the tracer correlations. The physical interpretation of the convective boundary condition in the mixing calculation is the mixing ratio of a tracer in an air mass injected by convection into the lower stratosphere. This convectively injected air mass is the starting point of the mixing calculation. As a

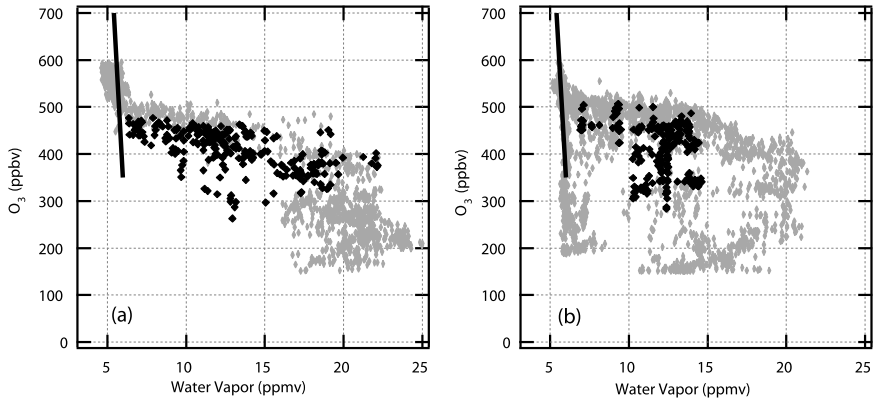

Figure 10. Correlations of ozone and water vapor for the flights of (left) 7 July and (right) 9 July 2002. Shading is the same as in Figure 5.

convective cloud rises through the troposphere, air is entrained at various levels, although mostly in the boundary layer, and mixes with the air in the cloud. Thus the convective boundary condition described here is roughly representative of the average composition over the depth of the convective entrainment level.

[29] Since the measurements included in the mixing calculation have elevated mixing ratios of tracers which are combustion products of biomass burning, the convective boundary conditions will be unusually high for those tracers. One tracer that is not significantly influenced by the biomass burning origin of the tropospheric air is water vapor. This is due to the fact that the mixing ratio of water vapor in the lower stratosphere is primarily determined by processes that occur near the tropopause. The processes that contribute to dehydration near the tropopause have been studied extensively, particularly in the tropics [*Jensen and Pfister*, 2004; *Gettelman et al.*, 2002], but it is still not clear what controls the amount of water vapor that enters the stratosphere. Subtropical and midlatitude convection is one of the processes that is thought to impact the humidity levels of air in the stratosphere, but has an uncertain role.

[30] Figure 10 shows correlations of water vapor versus ozone for the flights of 7 and 9 July. The plume correlations are much different from the typical lower stratospheric correlations as was seen for all the other tracers. The water vapor mixing ratios are much higher than the typical subtropical or midlatitude stratospheric value for a given O_3 mixing ratio, which suggests hydration of the lower stratosphere by the midlatitude convection. It is clear from Figure 10 that there are many other measured correlations besides those in the plume with relatively high water vapor mixing ratios for both of the flights. These correlations are more common in the high latitude lowermost stratosphere due to stratosphere-troposphere exchange, such as near the polar front jet, where relatively warm tropopause temperatures allow more water vapor to enter the stratosphere. Thus, in an air mass advected from high latitudes, correlations with high water vapor mixing ratios are not exclusively due to recent convection. We have used the other tracer correlations to identify the plume measurements that were most recently influenced by convection. The convective boundary condition for water vapor can be calculated in a similar manner as described in the previous section for the other tracers. This water vapor convective boundary condition is presumably representative of vigorous midlatitude convection that penetrates the lower stratosphere.

[31] Normalized distributions of the convective boundary conditions for CO, CO_2, NO_y and water vapor for the 7 and 9 July flights are shown in Figure 11. The CO distribution for both flights peaks between 200 and 300 ppbv, which is much higher than normal tropospheric mixing ratios, but well within the range of measurements taken in the troposphere downstream of forest fires [e.g., *Andreae et al.*, 2001]. NO_y and CO_2 also peak at significantly higher mixing ratios than normal tropospheric values in the Northern Hemisphere summer, consistent with the effects of biomass burning. Enhancements of trace gases in biomass burning plumes are commonly calculated by means of a ratio versus CO or CO_2 [e.g., *Mauzerall et al.*, 1998; *Andreae et al.*, 2001]. Since we assume the convection responsible for the plume injected a relatively fresh biomass burning air mass we can compare the enhancement ratios calculated from the convective boundary conditions to values from previous studies. The enhancement ratios are defined as $\Delta X/\Delta Y$, where ΔX represents the mixing ratio enhancement above a background level. Table 1 lists the basic PDF characteristics of the enhancement ratios calculated for both the 7 and 9 July flights. The enhancement ratio distributions generally fall within the range of values calculated from previous studies. This agreement with previous studies gives added confidence to the convective boundary condition calculation and further evidence for the rapid injection of a biomass burning plume into the stratosphere.

[32] The water vapor convective boundary condition distributions have interesting differences between the two flights. The 9 July distribution has peaks at 20 and 40 ppmv with no mixing ratios larger than 60 ppmv. The distribution from the 7 July flight is shifted somewhat toward higher water vapor mixing ratios with a main peak at 50 ppmv and some mixing ratios exceeding 80 ppmv. It is interesting to note that the small secondary peak at 15 ppmv in the 7 July distribution is entirely due to the plume measurements above 375 K on this date. Also, the 9 July peak at 40 ppmv is entirely due to

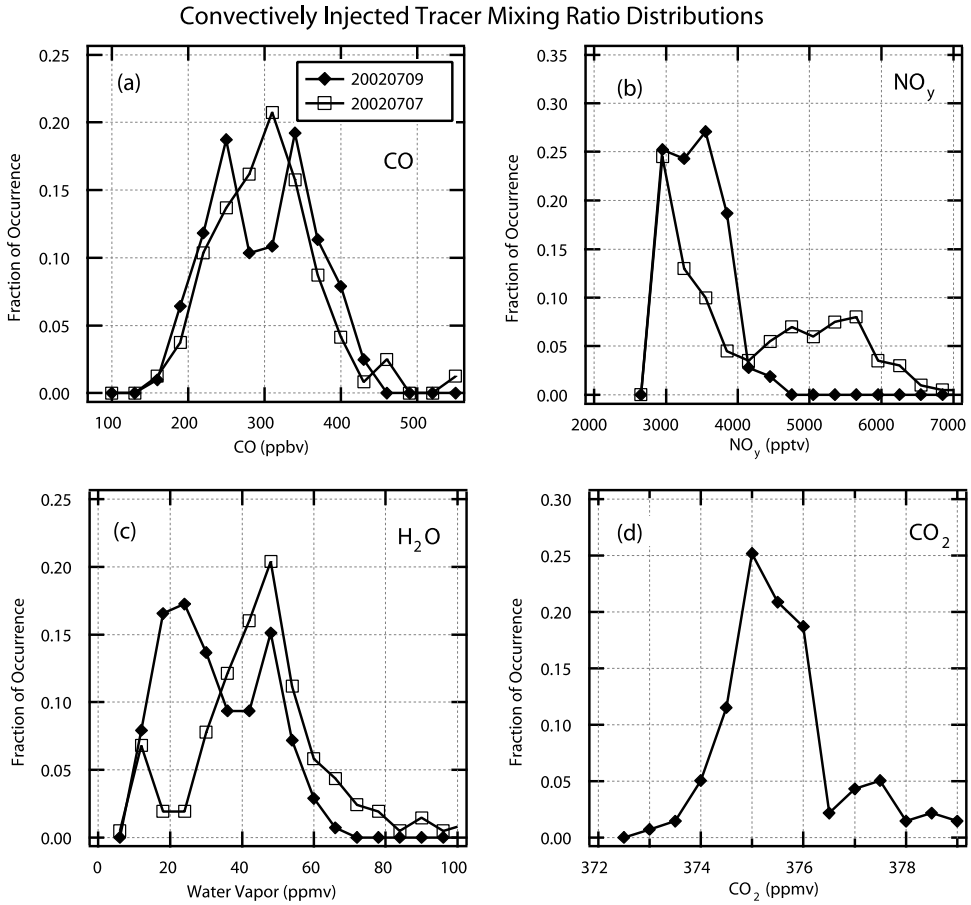

Figure 11. Normalized distributions of trace gas mixing ratios at the time the "plume" air mass was convectively injected into the lower stratosphere. The distributions are calculated from the measured mixing ratios in the lower stratospheric plume and the tropospheric fraction at the time of measurement determined from the mixing calculations as described in the text. Separate distribution for the flights of 7 and 9 July 2002 are shown for (a) CO, (b) NO_y, (c) water vapor, and (d) CO_2.

the plume measurements below 380 K on this date. Thus the convective boundary conditions for the two flights give a consistent picture of lower water vapor in air parcels lofted deeper into the stratosphere. All of the convectively injected water vapor mixing ratios for both flights are much larger than the background stratospheric values of 5–8 ppmv, which suggests substantial hydrating of the lower stratosphere by vigorous midlatitude convection.

[33] Since, as discussed in the previous section, we assume the plume from both flights was created from the same convective event then the different convective boundary conditions suggest that there was an inhomogeneous vertical distribution of tracers injected into the lower stratosphere. The difference in the water vapor distributions represents a vertical gradient in the amount of dehydration that occurred within the convective region. The high potential temperatures at which the plume was sampled on 9 July, and above 375 K on 7 July suggest this air was transported into the stratosphere by a very vigorous convective event or events. Since the local tropopause over the central United States was between 350 and 360 K, the convection and associated wave breaking and mixing above the convection penetrated well into the lower stratosphere. Convective plumes that penetrate well into the midlatitude stratosphere have been photographed by the ER-2 [*Roach*, 1967], inferred from satellite measurements [e.g., *Levizzani and Setvak*, 1996] and modeled [*Wang*, 2003]. However, in situ evidence of convective influence on the lower stratosphere up to 400 K has been limited to the tropics [*Danielsen*, 1993; *Kelly et al.*, 1993]. Thus, although there is plenty of evidence for the existence of vigorous midlatitude convection that penetrates deep into the lower stratosphere, the lack

Table 1. Plume Enhancement Ratios Calculated From the Convective Boundary Conditions[a]

	PDF Peak 7 July	80% Spread 7 July	PDF Peak 9 July	80% Spread 9 July	Previous Studies[b]
$\Delta NO_y/\Delta CO$	13	11–19	19	13–25	11–15
$\Delta NO_y/\Delta CO_2$	450	350–700	N/A	N/A	300–700
$\Delta CO/\Delta CO_2$	30	20–60	N/A	N/A	40–80

[a]The PDF peak represent the most probable value of the enhancement ratio and the 80% spread encompasses 80% of the values closest to the PDF peak. Units of NO_y are pptv, CO ppbv and CO_2 ppmv. Background mixing ratios used: NO_y = 750 pptv, CO = 100 ppbv, CO_2 = 371 ppmv (NOy estimated from tropospheric measurements during CRYSTAL-FACE and CO and CO_2 from CMDL flask measurements; see http://www.cmdl.noaa.gov/ccgg). N/A, not available.

[b]Data from *Mauzerall et al.* [1998] and *Andreae et al.* [2001].

of in situ measurements makes it difficult to determine the impact of this convection on the stratosphere. For instance, the modeling study of *Wang* [2003] showed that the convective plumes moistened the stratosphere but it is not known to what extent and whether the strength of the convection affects the amount of moistening. It is certainly not possible to make general conclusions based on two sampled events but the suggestion from the calculation performed here is that the convection was more effective at moistening the stratosphere just above the tropopause compared to the higher levels. However, in considering the impact of the convective moistening on the stratosphere as a whole, it is important to note that the vigorous convection moistened a large depth of the stratosphere, which subsequently was transported equatorward. The moistened air above 375 K is much more likely to rise into the tropical stratosphere and thus be circulated into the stratosphere as a whole by means of the Brewer-Dobson circulation, providing a potential influence on the middle and upper stratosphere.

[34] The estimates of the composition of air injected by convection into the stratosphere described above are likely to be somewhat unique due to the large amount of biomass burning material present. However, the mass of air injected into the stratosphere by convection may be more generally comparable to other convective events over the summertime continental United States. The convective mass flux likely plays a significant role in the budgets of water vapor and other trace gases in the extratropical lower stratosphere. Yet this quantity is very difficult to estimate through observations and is thus not well constrained. High-resolution models are beginning to resolve cloud processes with more accuracy [e.g., *Wang*, 2003], which makes observational estimates of convective mass flux quite important to constrain the models.

[35] We can estimate the mass of air injected into the stratosphere by the convective event responsible for the plume sampled on 9 July based on the plume size and the mixing fractions. This convective mass flux can be calculated by the equation $M = V \times \rho \times F$, where V is the volume of the plume at the time of sampling on 9 July, ρ is the average density of air in the plume and F is the average fraction of tropospheric air in the plume. To estimate the volume of the plume (V) we use the spatial information where the plume was sampled. Figure 12a shows a time series of CO and potential temperature and Figure 12b shows a portion of the flight track from the 9 July flight. The spikes in the CO time series signify where the plume above 375 K was intersected, as denoted by the symbols on the potential temperature curve. The sloping lines are drawn to roughly indicate the top and bottom vertical levels of the plume based on the multiple intersections. We would expect the plume to be sloping in the vertical due to the shear of the wind in the lower stratosphere. The northerly winds were stronger below 380 K compared to above 380 K based on NCEP wind fields (not shown). This would cause the lower levels of the plume to be advected further south than the upper levels, resulting in a sloping sheet. The observed transect through the plume is consistent with the wind shear characteristics since the higher levels of the plume were observed at later times, which are more northern locations on the return flight leg.

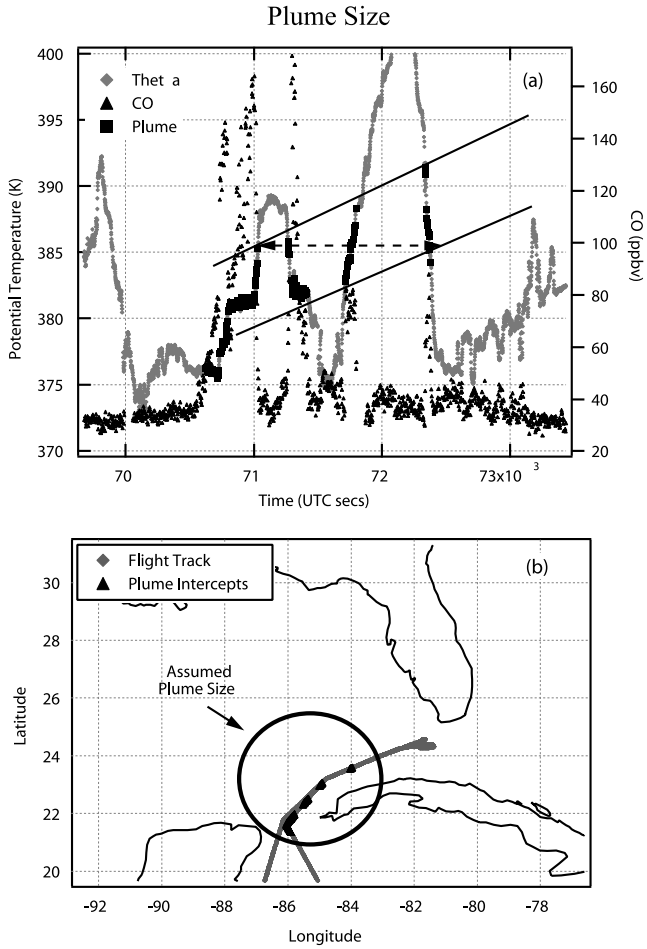

Figure 12. (a) Time series of potential temperature and CO from the 9 July 2002 flight. Points that are considered to be within the plume are overlaid on the potential temperature time series. The solid lines represent the sloping sheet of the plume. (b) Flight track of the 9 July flight with plume intercept points overlaid. The ellipse represents the assumed size of the plume based on the flight track and the wind shear.

[36] Since the WB-57F was traveling nearly in a straight line toward the northeast on the portion of the flight track considered here (Figure 12b), we can convert the plume intersections seen in the time series into a spatial scale. We can constrain the size of the plume based on an assumed potential temperature range of 375–395 K and the slope of the lines shown in Figure 12a. The lower boundary of 375 K is based on the fact that the outgoing leg of the 9 July flight followed the exact same track as the return leg over the region where the plume was sampled. Over this region on the outgoing leg, the WB-57F sampled up to 371 K without measuring any of the aerosol or trace gas plume characteristics described above. Figure 12b shows an elliptical approximation of the horizontal plume size based on the flight track intercepts. The plume is assumed to be elliptical in shape with a depth of 6 K potential temperature (Figure 12a), which corresponds to roughly 200 m in altitude. We take the average tropospheric fraction in the plume to be 0.25 based on the calculated values shown in Figure 9. Note

that we are only making this calculation for the upper level of the plume sampled on both 7 and 9 July above 375 K so this is an underestimate. These plume characteristics result in a convective mass injection of 5.6×10^{11} kg of air.

[37] We can compare this mass flux estimate to that calculated by *Wang* [2003] for a single thunderstorm over the midwestern United States. We use the water vapor flux estimate quoted in the paper, along with the lifetime and the water vapor mixing ratio of the modeled convective event to come up with an air mass flux of 1.3×10^{12} kg. This modeled mass flux is roughly two times larger than our estimate based on the sampled plume in the stratosphere. Considering the many possible differences in the two estimates, including variable convective strength, uncertainty in the plume size and mixing fraction among others, the agreement is reasonably good. It is almost certain that convective mass flux into the stratosphere varies by many orders of magnitude since it can range from near zero to the values shown above. However, the similarity in the modeled and observational estimates of mass injection suggests that a range of convective events in the summertime continental United States can impact the composition of the extratropical lower stratosphere, and perhaps the stratosphere as a whole.

4. Summary

[38] The unique sampling of the summer subtropical lower stratosphere by the WB-57F during the CRYSTAL-FACE mission has provided some insight into convective transport and mixing in this part of the atmosphere. We have taken advantage of the combination of abundant forest fires in the central United States and eastern Canada, the lofting of the smoke plumes into the lower stratosphere by vigorous convection and the southward advection in the lower stratosphere over the sampled region of Florida to examine stratospheric mixing. A key component in the ability to identify air that was recently transported from the troposphere into the stratosphere by convection as opposed to by some other process is the aerosol measurements of biomass burning particles [*Jost et al.*, 2004]. The aerosol signatures of biomass burning, along with anomalous trace gas measurements, clearly indicate the presence of recently injected tropospheric air in the stratosphere.

[39] We used measurements from the flights of 7 and 9 July 2002, when the most substantial smoke plumes were sampled, to make some simple calculations of mixing and the effects of convection on the subtropical lower stratosphere. Correlations of trace gases are used to calculate fractions of tropospheric air within the lower stratospheric plume. These fractions range from 0.1 up to nearly 0.5, which suggests that a portion of the plume maintained a significant signature of the troposphere as it was advected in the lower stratosphere for over a week. There is a distinct difference in the calculated mixing fractions above and below 375 K. These differences could be due to inhomogeneous mixing assuming the plume was created by a single convective event or convective strength differences assuming the plume was created by two nearly coincident events. We also estimated a range of mixing rates based on transit timescales of 7–12 days in the lower stratosphere between the convection and the time of sampling. These mixing rate estimates have a large uncertainty due to imprecise knowledge of the transit timescale as well as the amount of mixing that occurred during the convective event.

[40] The composition and mass of the input of tropospheric air into the stratosphere by convection is of interest due to the potential chemical and radiative impact on the stratosphere. From the mixing calculation we determined mixing ratio distributions of CO, NO_y, CO_2 and water vapor, at the time of convective input into the stratosphere. Most of the tracers were enhanced by regional biomass burning and thus their mixing ratio distributions are shifted toward higher mixing ratios compared to typical tropospheric values. Water vapor is different from the other tracers in that it is controlled primarily by the coldest temperatures within the cloud. The water vapor distributions from the measurements above and below 375 K are substantially different. The plume sampled above 375 K has a water vapor distribution shifted toward lower mixing ratios, with a peak from 15–20 ppmv, compared to the plume below 375 K, with a peak near 50 ppmv. Both of the water vapor mixing ratio distributions suggest that midlatitude convection moistens the extratropical lower stratosphere.

[41] If the distributions were created by the same convective event then this suggests an inhomogeneous vertical distribution of tracers injected into the lower stratosphere. The upper levels of the convective penetration into the stratosphere could be associated with colder temperatures through wave activity or perhaps increased particle fallout. While the lower levels of the convective penetration may inject moister air into the stratosphere, the upper levels may have more impact on the stratosphere as a whole. Since air above 360 K in the subtropics can rise in the upward branch of the mean stratospheric circulation the effect of the convection may be distributed into the stratosphere as a whole. Forward trajectories from the 9 July flight path (not shown) suggest that the sampled plume moved further south toward the equator where it was likely lifted into the tropical stratosphere. We also estimated the mass of tropospheric air injected into the stratosphere by the convection responsible for the plume above 375 K. The value of roughly 5.6×10^{11} kg is somewhat smaller than that calculated from a high-resolution cloud model. The substantial variability in extratropical convective strength and a lack of observational based estimates of convective mass injection into the stratosphere suggest a need for further study.

[42] The chance encounter of smoke plume air masses in the lower stratosphere during CRYSTAL-FACE discussed in this paper highlights yet again the importance of aircraft-based measurements in the UT/LS region. The high resolution and wide range of data taken from the aircraft can reveal features of the transport and chemistry that cannot be attained by other sampling platforms.

[43] **Acknowledgments.** We would like to thank the pilots and crew of the NASA WB-57F. Funding for this research was provided by a NASA Radiation Sciences Program grant.

References

Andreae, M. O., et al. (2001), Transport of biomass burning smoke to the upper troposphere by deep convection in the equatorial region, *Geophys. Res. Lett.*, *28*, 951–954.

Brasseur, G., and S. Solomon (1986), *Aeronomy of the Middle Atmosphere*, 2nd ed., D. Reidel, Norwell, Mass.

Danielsen, E. F. (1993), In situ evidence of rapid, vertical irreversible transport of lower tropospheric air into the lower tropical stratosphere

by convective cloud turrets and by large-scale upwelling in tropical cyclones, *J. Geophys. Res.*, *98*, 8665–8681.

Daube, B. C., Jr., K. A. Boering, A. E. Andrews, and S. C. Wofsy (2002), A high-precision fast-response airborne CO_2 analyzer for in situ sampling from the surface to the middle stratosphere, *J. Atmos. Oceanic Technol.*, *19*, 1532–1543.

Dunkerton, T. J. (1995), Evidence of meridional motion in the summer lower stratosphere adjacent to monsoon regions, *J. Geophys. Res.*, *100*, 16,675–16,688.

Esler, J. G., D. G. H. Tan, P. H. Haynes, M. J. Evans, K. S. Law, P.-H. Plantevin, and J. A. Pyle (2001), Stratosphere-troposphere exchange: Chemical sensitivity to mixing, *J. Geophys. Res.*, *106*, 4717–4731.

Fahey, D. W., et al. (1996), In situ observations of NO_y, O_3, and the NO_y/O_3 ratio in the lower stratosphere, *Geophys. Res. Lett.*, *23*, 1653–1656.

Fischer, H., et al. (2003), Deep convective injection of boundary layer air into the lowermost stratosphere at midlatitudes, *Atmos. Chem. Phys.*, *3*, 739–745.

Fromm, M. D., and R. Servranckx (2003), Transport of forest fire smoke above the tropopause by supercell convection, *Geophys. Res. Lett.*, *30*(10), 1542, doi:10.1029/2002GL016820.

Fromm, M. D., J. Alfred, K. Hoppel, J. Hornstein, R. Bevilacqua, E. Shettle, R. Servranckx, Z. Li, and B. Stocks (2000), Observations of boreal forest fire smoke in the stratosphere by POAM III, SAGE II, and lidar in 1998, *Geophys. Res. Lett.*, *27*, 1407–1410.

Gettelman, A., W. J. Randel, F. Wu, and S. T. Massie (2002), Transport of water vapor in the tropical tropopause layer, *Geophys. Res. Lett.*, *29*(01), 1009, doi:10.1029/2001GL013818.

Hintsa, E. J., et al. (1998), Troposphere-to-stratosphere transport in the lowermost stratosphere from measurements of H_2O, CO_2, N_2O and O_3, *Geophys. Res. Lett.*, *25*, 2655–2658.

Hoor, P., H. Fischer, L. Lange, J. Lelieveld, and D. Brunner (2002), Seasonal variations of a mixing layer in the lowermost stratosphere as identified by the CO-O_3 correlation from in situ measurements, *J. Geophys. Res.*, *107*(D5), 4044, doi:10.1029/2000JD000289.

Hudson, P. K., D. M. Murphy, D. J. Cziczo, D. S. Thomson, J. A. de Gouw, C. Warneke, J. Holloway, H. Jost, and G. Hübler (2004), Biomass-burning particle measurements: Characteristic composition and chemical processing, *J. Geophys. Res.*, *109*, D23S27, doi:10.1029/2003JD004398.

Jensen, E., and L. Pfister (2004), Transport and freeze-drying in the tropical tropopause layer, *J. Geophys. Res.*, *109*, D02207, doi:10.1029/2003JD004022.

Jost, H.-J., et al. (2004), In-situ observations of mid-latitude forest fire plumes deep in the stratosphere, *Geophys. Res. Lett.*, *31*, L11101, doi:10.1029/2003GL019253.

Kelly, K. K., A. F. Tuck, L. E. Heidt, M. Loewenstein, J. R. Podolske, S. E. Strahan, J. C. Wilson, and D. Kley (1993), Water vapor and cloud water measurements over Darwin during the STEP 1987 tropical mission, *J. Geophys. Res.*, *98*, 8713–8724.

Lane, T. P., R. D. Sharman, T. L. Clark, and H.-M. Hsu (2003), An investigation of turbulence generation mechanisms above deep convection, *J. Atmos. Sci.*, *60*, 1297–1321.

Lelieveld, J., B. Bregman, F. Arnold, V. Burger, P. J. Crutzen, H. Fischer, A. Waibel, P. Siegmund, and P. F. J. van Velthoven (1997), Chemical perturbation of the lowermost stratosphere through exchange with the troposphere, *Geophys. Res. Lett.*, *24*, 603–606.

Levizzani, V., and M. Setvak (1996), Multispectral, high-resolution satellite observations of plumes on top of convective storms, *J. Atmos. Sci.*, *53*, 361–369.

Loewenstein, M., H.-J. Jost, J. Grose, J. Eilers, D. Lynch, S. Jensen, and J. Marmie (2002), ARGUS: A new instrument for the measurement of the stratospheric dynamical tracers, N_2O and CH_4, *Spectrochim. Acta*, *58*(11), 2329–2345.

Mauzerall, D. L., J. A. Logan, D. J. Jacob, B. E. Anderson, D. R. Blake, J. D. Bradshaw, B. Heikes, G. W. Sachse, H. Singh, and B. Talbot (1998), Photochemistry in biomass burning plumes and implications for tropospheric ozone over the tropical South Atlantic, *J. Geophys. Res.*, *103*, 8401–8423.

Murphy, D. M., D. S. Thomson, and M. J. Mahoney (1998), In situ measurements of organics, meteoritic material, mercury, and other elements in aerosols at 5 to 19 km, *Science*, *282*, 1664–1669.

Plumb, R. A., and M. K. W. Ko (1992), Interrelationships between mixing ratios of long-lived stratospheric constituents, *J. Geophys. Res.*, *97*, 10,145–10,156.

Plumb, R. A., W. Heres, J. L. Neu, N. M. Mahowald, J. del Corral, G. C. Toon, E. Ray, F. Moore, and A. E. Andrews (2002), Global tracer modeling during SOLVE: High-latitude descent and mixing, *J. Geophys. Res.*, *107*, 8309, doi:10.1029/2001JD001023 [printed 108 (D5), 2003].

Proffitt, M. H., and R. L. McLaughlin (1983), Fast-response dual-beam UV-absorption ozone photometer suitable for use in stratospheric balloons, *Rev. Sci. Instrum.*, *54*, 1719–1728.

Ray, E. A., F. L. Moore, J. W. Elkins, G. S. Dutton, D. W. Fahey, H. Vomel, S. J. Oltmans, and K. H. Rosenlof (1999), Transport into the Northern Hemisphere lowermost stratosphere revealed by in situ tracer measurements, *J. Geophys. Res.*, *104*, 26,565–26,580.

Ray, E. A., F. L. Moore, J. W. Elkins, D. F. Hurst, P. A. Romashkin, G. S. Dutton, and D. W. Fahey (2002), Descent and mixing in the 1999–2000 northern polar vortex inferred from in situ tracer measurements, *J. Geophys. Res.*, *107*(D20), 8285, doi:10.1029/2001JD000961.

Richard, E. C., K. C. Aikin, E. A. Ray, K. H. Rosenlof, T. L. Thompson, A. Weinheimer, D. Montzka, D. Knapp, B. Ridley, and A. Gettelman (2003), Large-scale equatorward transport of ozone in the subtropical lower stratosphere, *J. Geophys. Res.*, *108*(D23), 4714, doi:10.1029/2003JD003884.

Ridley, B. A., J. G. Walega, J. E. Dye, and F. E. Grahek (1994), Distribution of NO, NO_x, NO_y and O_3 to 12 km altitude during the summer monsoon season over New Mexico, *J. Geophys. Res.*, *99*, 25,519–25,534.

Roach, W. T. (1967), On the nature of the summit areas of severe storms in Oklahoma, *Q. J. R. Meteorol. Soc.*, *93*, 318–336.

Rosenlof, K. H. (1995), Seasonal cycle of the residual mean meridional circulation in the stratosphere, *J. Geophys. Res.*, *100*, 5173–5191.

Ryerson, T. B., et al. (2001), Observations of ozone formation in power plant plumes and implications for ozone control strategies, *Science*, *292*, 719–723.

Thompson, T. L., and K. H. Rosenlof (2003), Accuracy and precision of the NOAA Aeronomy Laboratory pressure temperature instrument on the NASA WB-57F, poster presented at CRYSTAL-FACE Science Team Meeting, NASA, Salt Lake City, Utah. (available as http://cloud1.arc.nasa.gov/crystalface/presentations_files/1-34_Rosenlof&Thompson.pdf)

Tuck, A. F., et al. (1997), The Brewer-Dobson circulation in the light of high altitude in situ aircraft observations, *Q. J. R. Meteorol. Soc.*, *123*, 1–69.

Waibel, A. E., H. Fischer, F. G. Wienhold, P. C. Siegmund, B. Lee, J. Strom, J. Lelieveld, and P. J. Crutzen (1999), Highly elevated carbon monoxide concentrations in the upper troposphere and lowermost stratosphere at northern midlatitudes during the STREAM II summer campaign in 1994, *Chemosphere Global Change Sci.*, *1*, 233–248.

Wang, P. K. (2003), Moisture plumes above thunderstorm anvils and their contributions to cross-tropopause transport of water vapor in midlatitudes, *J. Geophys. Res.*, *108*(D6), 4194, doi:10.1029/2002JD002581.

D. J. Cziczo, P. K. Hudson, E. A. Ray, E. C. Richard, and K. H. Rosenlof, NOAA Aeronomy Laboratory, MS R/AL6, 325 Broadway, Boulder, CO 80305, USA. (eray@al.noaa.gov)

B. C. Daube, C. Gerbig, S. C. Wofsy, and I. Xueref, Department of Atmospheric Sciences, Harvard University, 29 Oxford Street, Cambridge, MA 02138, USA.

R. L. Herman, Jet Propulsion Laboratory, MS 183-401, 4800 Oak Grove Drive, Pasadena, CA 91109, USA.

H.-J. Jost, M. Loewenstein, and J. Lopez, NASA Ames Research Center, Mail Stop 245-5, Moffett Field, CA 94035-1000, USA.

D. Knapp, D. Montzka, B. Ridley, and A. Weinheimer, National Center for Atmospheric Research, 1850 Table Mesa Drive, Boulder, CO 80307, USA.